EUROPEAN ORGANIZATION FOR NUCLEAR RESEARCH

Antinuclei from $\overline{\Lambda}_{\mathrm{b}}$ decays

R. Ferioli[1]

Email: roberta.ferioli@edu.unito.it

Supervisors: F. Mazzaschi[2], I. Vorobyev[2]

1. University of Turin
2. European Organisation for Nuclear Research (CERN)

Abstract

Light antinuclei in space such as antideuterons and antihelium-3 are considered as one of the most promising probes for indirect dark-matter searches, because astrophysical production via convenient Standard Model processes is expected to be extremely low. Recent observations by the Alpha Magnetic Spectrometer of a handful of tentative antihelium events have triggered a lot of discussions about their potential origin. Among them the production of antihelium through the decays of $\overline{\Lambda}_{\mathrm{b}}$ baryons was demonstrated to be able to significantly boost the antihelium flux in space. However, the branching ratio of $\overline{\Lambda}_{\mathrm{b}} \rightarrow^3 \overline{\mathrm{He}} + X$ process is not known from the experiment, which can significantly affect the resulting antihelium flux. In this project, we use the ALICE detector capabilities to search for the antihelium nuclei from displaced vertex of $\overline{\Lambda}_{\mathrm{b}}$ decays with the Run 3 pp data. The distance of closest approach of antihelium nuclei is fitted with various templates that include the $\overline{\Lambda}_{\mathrm{b}} \rightarrow^3 \overline{\mathrm{He}} + X$, which can be used to directly constrain the inclusive $\overline{\Lambda}_{\mathrm{b}} \rightarrow^3 \overline{\mathrm{He}} + X$ branching ratio. The analysis techniques are first validated and tested by looking at the antideuteron nuclei that can also come from the decays of $\overline{\Lambda}_{\mathrm{b}}$ baryon.

1   Introduction

The presence of light antinuclei (such as antideuteron or antihelium) in space remains one of the most intriguing questions of modern physics. Many theoretical predictions suggest that such antinuclei can originate from exotic processes such as dark matter (DM) annihilations and decays. The corresponding antinuclei flux near Earth is expected to exceed the background from ordinary standard model processes by orders of magnitude in the low kinetic energy range, making the observation of such antinuclei in space a smoking gun for new exotic physics.

The AMS-02 experiment has announced the potential detection of $\mathcal{O}(10)$ $^3\overline{\text{He}}$ events, along with $\mathcal{O}(1)$ potential $^4\overline{\text{He}}$ events [1]. However, dark-matter models are expected to produce $\ll 1$ detectable $^3\overline{\text{He}}$ event [2]. One possible explanation might be the $^3\overline{\text{He}}$ from $\overline{\Lambda}_b$ baryon decays produced in dark-matter annihilation [3]. In support of this statement we can consider that $\overline{\Lambda}_b$ baryons (and other unstable bottom hadrons) are generically produced in dark matter annihilation channels involving b quarks. However, $\overline{\Lambda}_b$ is uniquely important because it has an antibaryon number, and a 5.6 GeV rest mass which lies just above the 4.7 GeV rest mass of three stable antibaryons and two stable baryons (e.g., two antiprotons, an antineutron, and two protons). Thus, if a $\overline{\Lambda}_b$ decays to such a state and the decay products have small relative momenta in the $\overline{\Lambda}_b$ rest frame, this would allow for a coalescence of antibaryons into antihelium. Fig. 1 shows the antihelium flux from dark-matter annihilation using different event generators that include $\overline{\Lambda}_b \rightarrow^3 \overline{\text{He}} + X$ decays.
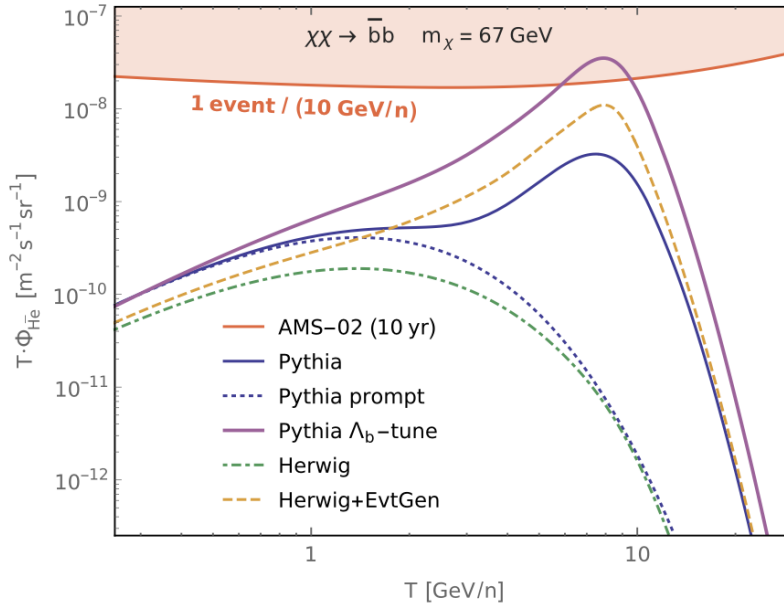

Fig. 1: Antihelium flux from dark-matter annihilation for different cases of $\overline{\Lambda}_b \rightarrow^3 \overline{\text{He}} + X$ decays. The so-called Pythia $\overline{\Lambda}_b$ tune (purple line) boosts the antihelium flux so that it reaches the AMS-02 sensitivity (red area). Figure is taken from [3].

Only the purple line, called "Λ_b-tune", reaches the red area representing the AMS-02 sensitivity of 10-year data taking. It considers a BR($\overline{\Lambda}_b \rightarrow^3 \overline{\text{He}} + X$) which is as high as $3 * 10^{-6}$; however, this value remains unknown from the experiment. At LHC it is possible to look for $\overline{\Lambda}_b$ decaying to $^3\overline{\text{He}}$ and to constrain this BR from the experimental point of view. Also $\overline{\text{d}}$ can come from $\overline{\Lambda}_b$, but in this case there is also the feed-down from B meson ($\overline{B^0}/\overline{B^+}/\overline{B_s^0} \rightarrow \overline{d} + X$).

This projects aims at searching for the antinuclei coming from the beauty hadron decays produced in pp collisions at the LHC. The characteristic distribution of the selected pure antinuclei over their Distance

of Closest Approach (DCA) to the primary vertex helps to distinguish between the antinuclei originating from the primary collision vertex and those coming from displaced beauty hadron decays. $\overline{\Lambda}_b$ has $c\tau \sim 420\ \mu$m so the decay products won't point to the primary vertex. For this reason, the distribution of the Distance of the Closest Approach in the plane perpendicular to the beam axis (DCA_{xy}) of antinuclei from $\overline{\Lambda}_b$ is expected to be wider than the primary ones. The DCA resolution of ITS is $\sim 20\ \mu$m (at the transverse momentum of $p_T = 1.5$ GeV/c), so low enough to see the difference in DCA distributions. A schematic representation of this difference in DCA values is shown in Figure 2. The DCA distribution is characterised with the templates obtained from Monte Carlo simulations in different ranges of the antinuclei transverse momentum (p_T). The analysis procedure is first benchmarked and tested with antideuterons, before the DCA distribution of antihelium-3 nuclei are analysed.
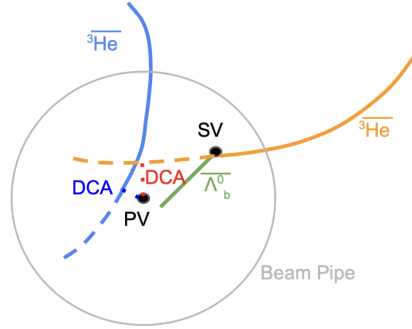
Fig. 2: Schematic representation of $^3\overline{\text{He}}$ tracks and their DCA for primary $^3\overline{\text{He}}$ (blue) and for $^3\overline{\text{He}}$ from $\overline{\Lambda}_b$ (orange).

2 The ALICE experiment

2.1 The Large Hadron Collider

The Large Hadron Collider (LHC) is the final component of CERN accelerator complex, which progressively accelerates particles to higher energies. Each machine in this chain increases the energy of a particle beam and then injects it into the next machine. Protons and heavy ions are brought to their collision energies through different acceleration chains. In 2022 the LHC started its third data taking period, the so-called Run 3, which is expected to be continued until the end of 2025.

2.2 ALICE

A Large Ion Collider Experiment (ALICE) is one of the four experiments installed at the LHC. ALICE was designed and built to study a phase of matter called the Quark Gluon Plasma, which is formed in heavy-ion collisions at ultra-relativistic energies. For this purpose, it is necessary to track and to identify all the particles produced in heavy-ion collisions (^{208}Pb). ALICE is also studying proton-proton and proton-nucleus collisions both as a comparison with nucleus-nucleus collisions and in their own right.

To provide a comprehensive set of measurements to study the properties of the QGP, detectors with high granularity and fast readout capabilities are needed. The ALICE detector was designed to meet these requirements. The two main detectors used in this work are:

– **the Inner Tracking System (ITS)**: the innermost detector of the ALICE apparatus, which is designed to provide precise tracking and vertex reconstruction in the high-multiplicity environment of heavy-ion collisions. The current version of ITS is called ITS2 and is composed of 7 layers of silicon detectors based on the Monolithic Active Pixel Sensors technology [4]
– **the Time Projection Chamber (TPC):** the main tracking device used for tracking of charged particles and particle identification. It is a 90 m^3 cylinder filled with gas and divided in two drift regions by the central electrode located at its axial centre. It is designed to provide particle

identification via dE/dx of charged particles [5]. Figure 3 shows the specific energy loss in the TPC gas from pp 13.6 TeV data.
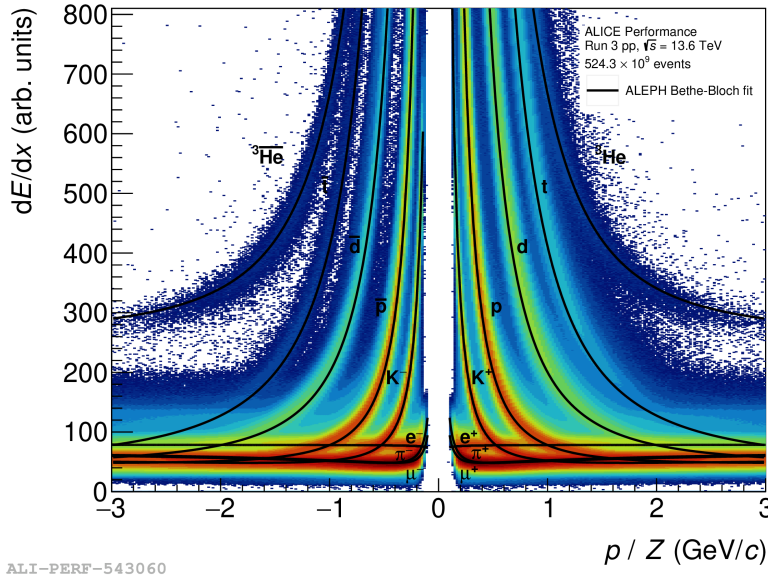
Fig. 3: Specific energy loss in the ALICE TPC in pp 13.6 TeV data. The Bethe-Bloch parameterisations for different particle species are shown as black lines. The $^3\overline{\text{He}}$ nuclei are well separated from lighter particles over a large momentum range thanks to their double charge and large mass.
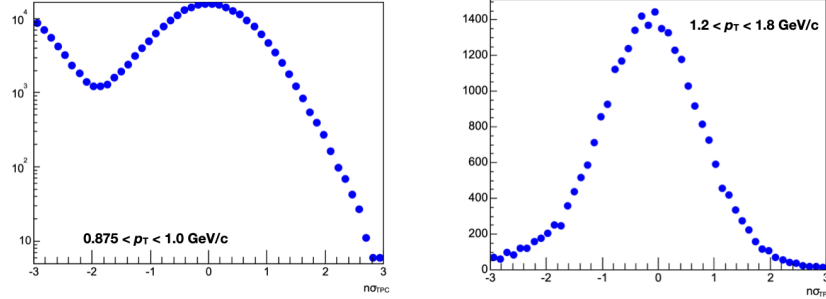
3 Analysis

The goals of this project are:

- to obtain the templates to characterize the DCA distributions of antinuclei from different sources using MC simulations
- to develop the machinery to fit the DCA distribution of antinuclei in experimental data with all relevant DCA templates
- to study the feasibility of the search for antinuclei from $\overline{\Lambda}_b$ decays with ITS2

For this work the Run 3 pp data at $\sqrt{s} = 13.6$ GeV/c collected in 2023 and 2024 are used, together with MC simulation of pp events with $\sqrt{s} = 13.6$ GeV/c and a simulation of $\overline{\Lambda}_b \to^3 \overline{\text{He}} + X$ with Pythia8. The track selection used in this work is reported in table 1. This selection ensures a high quality of reconstructed charged-particle tracks and a high purity of antihelium candidates in the TPC.

Table 1: Track selection used in analysis

Variable	Requirement
η	$|\eta| < 1.0$
rapidity	$|\eta| < 0.5$
N of TPC clusters	≥ 90
N of ITS clusters	≥ 6
Distance of closest approach in xy plane	$\text{DCA}_{xy} \leq 0.05$ cm
Distance of closest approach in z direction	$\text{DCA}_z \leq 0.05$ cm
N of sigmas TPC	$|n\sigma_{TPC}| \leq 3$

Figure 4 shows the $n\sigma_{TPC}$ distributions[1] for $\overline{d}$ and $^3\overline{He}$ at relatively low p_T. As we can see, for $^3\overline{He}$ there is no background from misidentified particles. This is because, as can be seen in figure 3, $^3\overline{He}$ thanks to their charge[2] is well separated from others particles unlike $\overline{d}$ which are well separated only at low momentum. The corresponding background for $\overline{d}$ is clearly seen in Fig. 4 (left), which should be taken into account during the DCA fit procedure.

Fig. 4: Comparison of $n\sigma_{TPC}$ distribution for $\overline{d}$ (left) and $^3\overline{He}$ (right) at low p_T.

In the following, first the validation of the analysis procedure with antideuterons is described, after which the results for antihelium-3 are reported.

3.1   Different contributions to DCA_{xy} distribution of antideuterons

The DCA_{xy} distribution that can be observed in experimental data includes several contributions. It is necessary know all of them before trying to fit the data. In addition to the antinuclei coming from $\overline{\Lambda}_b$ decays, the list of contributions to be considered is given below:

– Primary antinuclei, i.e. antinuclei originating from primary pp collision vertex
– Decays of $^3_\Lambda\overline{H}$
– Residual background, which includes misidentified antinuclei (only for $\overline{d}$) and antinuclei from wrongly associated collisions during the event and track reconstruction

For $\overline{d}$ it is necessary to take care of other particles misidentified as $\overline{d}$. The template of this contribution was taken from the sideband region (-3,-2) of the $n\sigma_{TPC}$ (light blue area in figure 5 in the left plot), assuming that the DCA_{xy} distribution of the background is the same in sideband region and under the signal peak. In figure 5 in the right plot the corresponding DCA_{xy} template is shown.
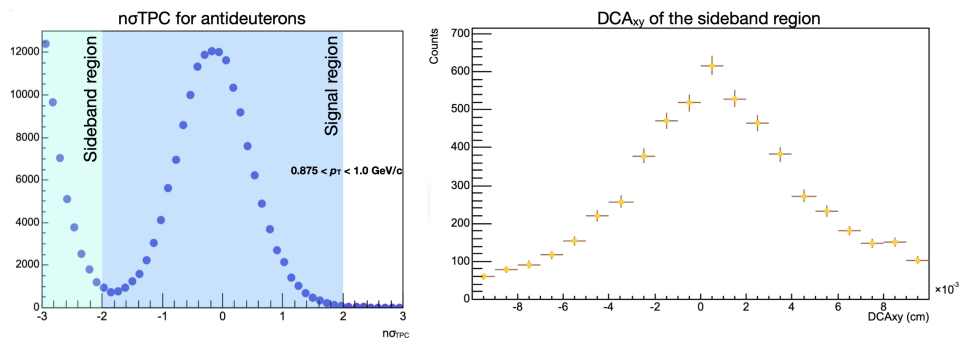
Fig. 5: Different region of $n\sigma_{TPC}$ distribution used to define the signal and the sideband areas (left), and the background DCA_{xy} template from sideband (right).

---

[1] $n\sigma_{TPC}$ is the ratio of the difference in measured and expected TPC signal to the width of the signal distribution (it is assumed that it is 9% (6% for $^3\overline{He}$) of the expected value)

[2] According to Bethe-Bloch formula the dE/dx goes as z^2
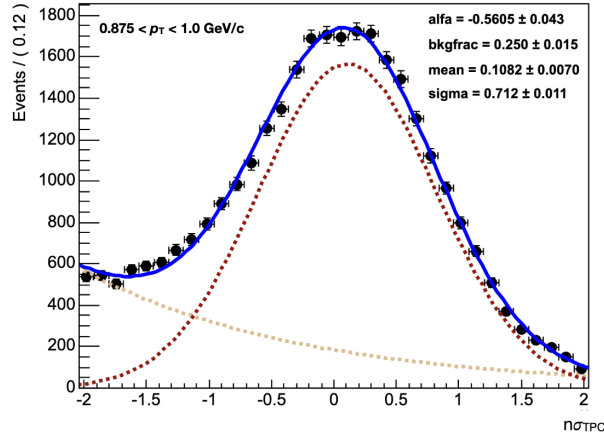
Fig. 6: Fit of nσ_{TPC} distribution in the signal region. In blue the total fit, in dark brown the signal and in lighter brown the background components are shown.

To fix the correct fraction of this type of background in the signal region ((-2,2), dark blue area in figure 5), the nsigmaTPC distribution has been fitted with a two-component function that includes a gaussian for the signal and exponential function for the background using RooFit [6] library (Fig. 6). The background fraction in the DCA_{xy} fit is fixed to the one obtained from the fit to nsigmaTPC.

The others contributions are the template of the primary tracks, matched with correct collision, the template of the $\bar{d}$ from $^{3}_{\Lambda}\overline{H}$ decay and the template of the primary tracks associated with wrong collision. All three templates are obtained with the help from MC simulations. These template are reported in figure 7.
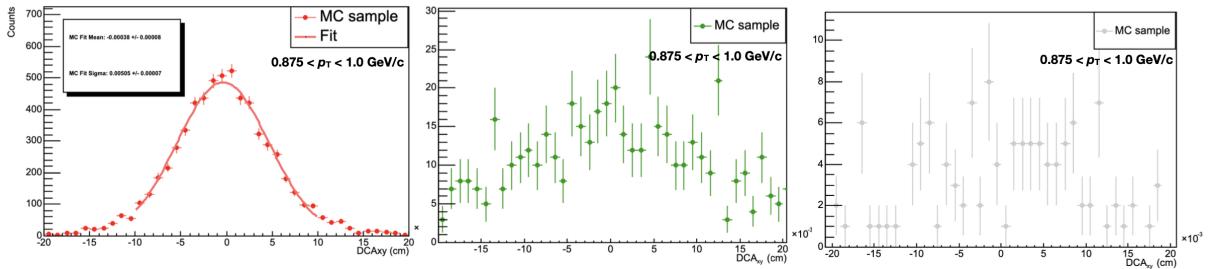

Fig. 7: DCA_{xy} templates for $\bar{d}$ from MC simulation. Template of primary matched $\bar{d}$ with the correct collision id is shown in red, the template of $\bar{d}$ from $^{3}_{\Lambda}\overline{H}$ in green, and the template of primary tracks matched with wrong collision in gray.

3.2   MC closure test for antideuterons

To check the self-consistency of the analysis method and the presence of potential bias a so-called MC closure test has been performed for $\bar{d}$ MC data. It is a procedure in which MC reconstructed data is processes used both the MC truth information (to get pure primary $\bar{d}$) and is also processed just like experimental data (i.e. including background from misidentified particles). The $DCAxy$ distribution is fitted with all the template listed before. The σ and the mean of the gaussian signal peak are left free as well as the fraction of $\bar{d}$ from $^{3}_{\Lambda}\overline{H}$ and the fraction of primary tracks matched with wrong collision, whereas the mean and the σ of the background from misidentified particles are fixed. If the procedure works properly, the σ of the gaussian and the fractions obtained from the fit in Fig. 8 will be comparable with the ones from the fit to $\bar{d}$ that are selected with the MC truth information.

As shown in figure 9, the sigma taken from the fit with all components (in black) is comparable to the one from the fit using MC truth information. This is also true for the fraction of $\bar{d}$ from $^{3}_{\Lambda}\overline{H}$ and the fraction of $\bar{d}$ matched with wrong collision as we can see in table 2. These results demonstrate the self-consistency
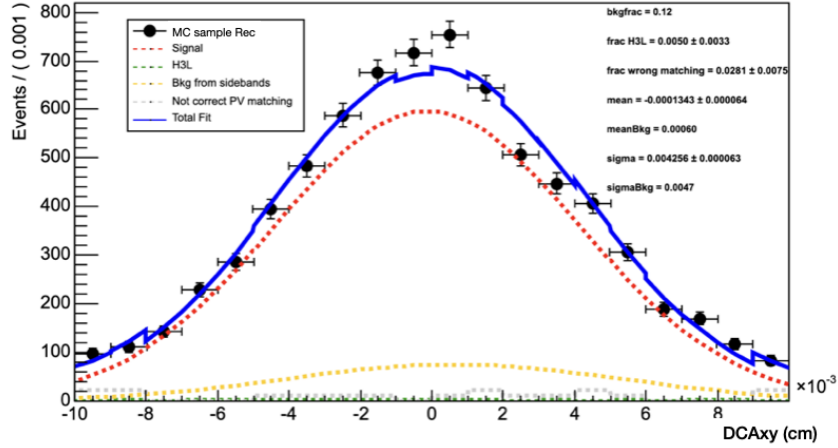
Fig. 8: Fit to $\overline{\text{d}}$ *DCAxy* distribution in MC reconstructed data. In blue the total fit, in red the signal, in yellow the background from misidentified particles, in green the $\overline{\text{d}}$ from $^3_\Lambda\overline{\text{H}}$, in gray the primary tracks matched with the wrong collision.

of the used method, therefore it is possible to proceed with the analysis of real data.
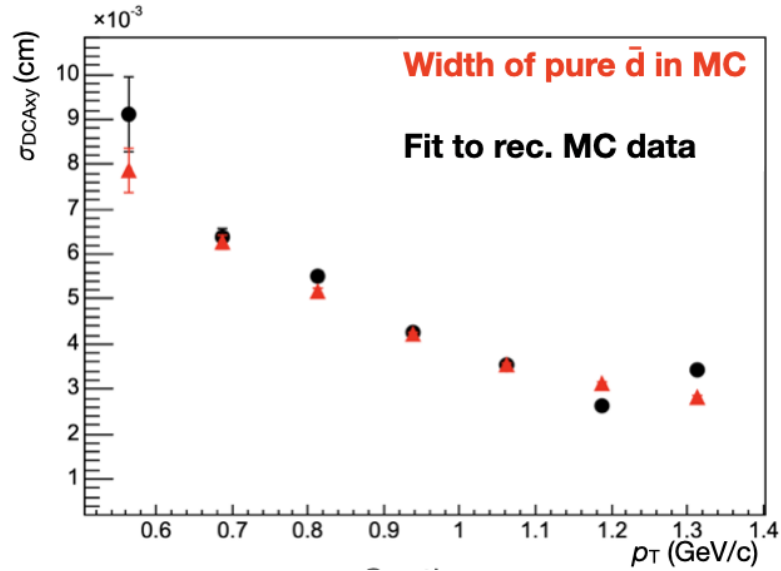
Fig. 9: σ of the DCA_{xy} vs p_T. In black the σ of the gaussian taken from the fit in figure 8, in red the σ of the distribution of $\overline{\text{d}}$ selected with the MC truth information.

3.3 Tuning the MC sample

To properly fit the data it is necessary that the resolution of the DCA_{xy} distribution in MC simulation and in data are the same. In the current Run 3 data the resolution observed in experimental data is wider than in MC. While a better reconstruction of the experimental data is a more challenging task that goes beyond the scope of the current project, it is possible to "worsen" the MC simulation to match the resolution observed in experimental data. In order to do that, a tool called "Track tuner" which smears the track parameter of MC tracks and consequently the smearing of DCA_{xy} distribution, has been added to the analysis task. In figure 10 the values of the σ of the DCA_{xy} distribution are shown as a function of p_T. It can be seen that after applying track tuner (darker red points) the values of $\sigma_{DCA_{xy}}$ are closer to the ones observed in data (blue points). For $\overline{\text{d}}$ there is a good agreement between data and MC after applying track tuner, while for $^3\overline{\text{He}}$ there is a significant improvement which is however not enough to completely

	MC truth Fraction	Fit Fraction
$\bar{\mathrm{d}}$ from $^3_\Lambda\overline{\mathrm{H}}$	0.003	0.005 ± 0.003
$\bar{\mathrm{d}}$ matched with wrong collision	0.027	0.028 ± 0.007

Table 2: Fraction of $\bar{\mathrm{d}}$ from $^3_\Lambda\overline{\mathrm{H}}$ and of the matched with wrong collision

eliminate the difference between data and MC. A possible explanation of this discrepancy is the double charge of $^3\overline{\mathrm{He}}$, as this give an extra curvature to the tracks. This imperfect agreement between MC and data could create biases when the latter will be fitted.
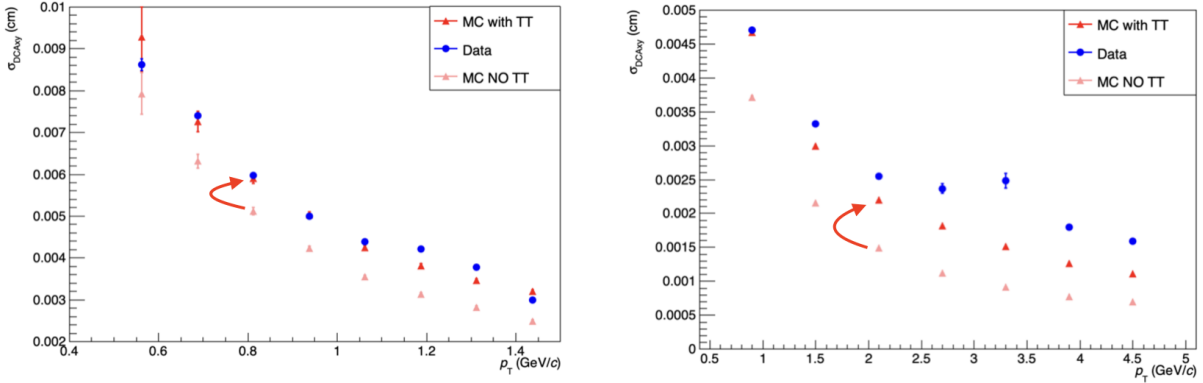
Fig. 10: σ of DCA_{xy} vs p_T for data (blue), MC without (lighter red) and with (darker red) track tuner for $\bar{\mathrm{d}}$ (left) and $^3\overline{\mathrm{He}}$ (right). The effect of track tuner is shown as a red arrow.

3.4 $\overline{\Lambda_b} \to\, ^3\overline{\mathrm{He}}$ contributions to DCA_{xy} distribution of $^3\overline{\mathrm{He}}$

For this work, the DCA_{xy} template of $^3\overline{\mathrm{He}}$ from $\overline{\Lambda_b} \to\, ^3\overline{\mathrm{He}}$ is taken from Pythia8 simulation that was performed in the scope of the studies for the ALICE3 Letter of Intent [7]. In [7] it is assumed that the templates of $^3\overline{\mathrm{He}}$ from $\overline{\Lambda_b}$ and the one of $^3\overline{\mathrm{He}}$ from $^3_\Lambda\overline{\mathrm{H}}$ are the same at low momentum, which is the worst-case scenario for the analysis of $^3\overline{\mathrm{He}}$ from $\overline{\Lambda_b}$. However, as can be seen from 11, the two templates are quite different at low momentum, and become compatible only at $p_T > 3$ GeV/c.
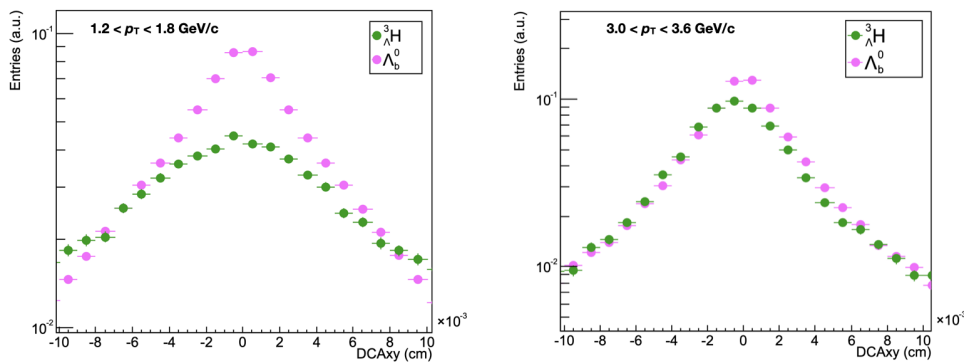

Fig. 11: Template of $^3\overline{\mathrm{He}}$ from $\overline{\Lambda_b}$ (magenta) and $^3\overline{\mathrm{He}}$ from $^3_\Lambda\overline{\mathrm{H}}$ (green). On the left in the region $1.2 < p_T < 1.8$, on the right $3.0 < p_T < 3.6$.

4 Results

As a last step, the $^3\overline{\mathrm{He}}$ data have been fitted by adding all the different templates described above. The σ of the primary template and the fraction of the tracks matched with wrong collision are fixed from MC simulations. The fraction of $^3\overline{\mathrm{He}}$ from $^3_\Lambda\overline{\mathrm{H}}$ is fixed to 1.5 % relative to the primary contribution according
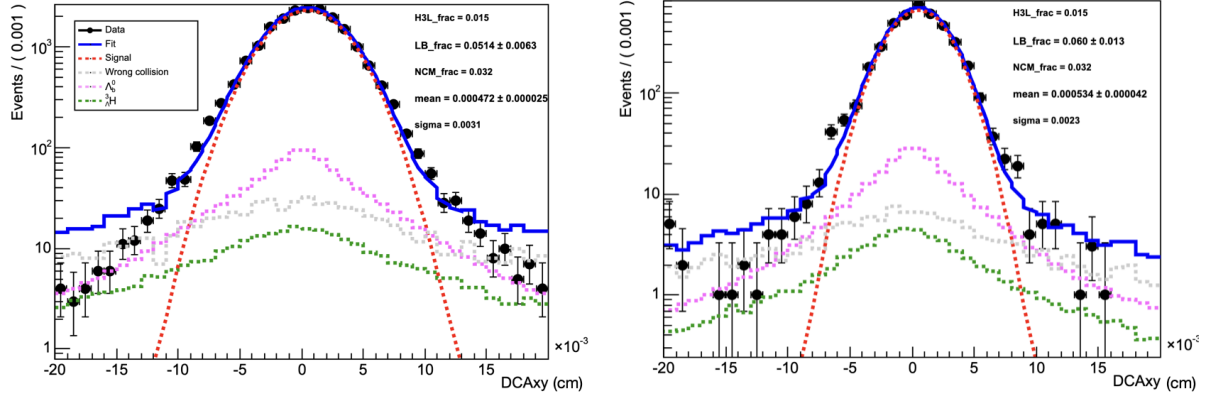
Fig. 12: DCA_{xy} distribution of $^3\overline{\mathrm{He}}$ fitted whit all relevant templates obtained from the MC simulation in $1.2 < p_T < 1.8$ GeV/c (left) and in $1.8 < p_T < 2.4$ GeV/c (right). In blue the total fit, in red the primary signal, in green $^3\overline{\mathrm{He}}$ from $^3_{\Lambda}\overline{\mathrm{H}}$, in pink $^3\overline{\mathrm{He}}$ from $\overline{\Lambda}_b$ and in gray the primary tracks matched with the wrong collision are shown.

to [7]. The template of $^3\overline{\mathrm{He}}$ from $\overline{\Lambda}_b$ is taken from the Pythia8 simulation, and its fraction is left free. In figure 12 the total fit in two different momentum ranges of $1.2 < p_T < 1.8$ GeV/c and $1.8 < p_T < 2.4$ GeV/c is shown. The fraction of $^3\overline{\mathrm{He}}$ from $\overline{\Lambda}_b$ obtained from the fit is (0.051 ± 0.006) for the first bin and (0.060 ± 0.013) for the second bin.

5   Summary and outlook

In this work I have developed the machinery for fitting the antinuclei DCA distributions with all needed templates to study for the first time the antinuclei originating from beauty decays in the ALICE experimental data. As a part of these efforts, the usage of track tuner helper task was implemented and tested in the analysis code, which improved the description of DCA distributions in experimental data by the MC simulations. The self-consistency of the analysis procedure was demonstrated with antideuterons, after which the analysis techniques have been applied to the experimental data of antihelium-3 nuclei. The preliminary results show that it is in principle possible to search for antinuclei from $\overline{\Lambda}_b$ decays, however several aspects of the analysis can be improved in the future. First, it is necessary to better describe the shape of different templates and their contributions to the total yield. The track tuner for $^3\overline{\mathrm{He}}$ has to be improved for a better description of experimental data resultion with MC simulation. The $^3\overline{\mathrm{He}}$ from $\overline{\Lambda}_b$ template should be updated with the actual performance of ITS2 detector[3]. The fraction of $^3\overline{\mathrm{He}}$ from $^3_{\Lambda}\overline{\mathrm{H}}$ can be updated based on the ALICE Run 3 MC simulations. Last but not least, it is also necessary to collect more statistics to improve the limits on the BR as it is shown in Fig. 73 from [7].

---

[3]The one used in this work is taken from a simulation assuming nominal ITS2 performance that was produced before the start of Run 3 data taking

References

[1] S. Ting, "Latest results from ams on the international space station (iss)", 2023. `https://indico.cern.ch/event/1275785/`.

[2] V. Poulin, P. Salati, I. Cholis, M. Kamionkowski, and J. Silk, "Where do the AMS-02 antihelium events come from?", *Phys. Rev. D* **99** (2019) 023016, `arXiv:1808.08961 [astro-ph.HE]`.

[3] M. W. Winkler and T. Linden, "Dark Matter Annihilation Can Produce a Detectable Antihelium Flux through $\bar{\Lambda}_b$ Decays", *Phys. Rev. Lett.* **126** (2021) 101101, `arXiv:2006.16251 [hep-ph]`.

[4] **ALICE** Collaboration, S. Acharya *et al.*, "ALICE upgrades during the LHC Long Shutdown 2", *JINST* **19** (2024) P05062, `arXiv:2302.01238 [physics.ins-det]`.

[5] J. Alme *et al.*, "The ALICE TPC, a large 3-dimensional tracking device with fast readout for ultra-high multiplicity events", *Nucl. Instrum. Meth. A* **622** (2010) 316–367, `arXiv:1001.1950 [physics.ins-det]`.

[6] "Roofit manual." `https://root.cern/manual/roofit/`.

[7] **ALICE** Collaboration, "Letter of intent for ALICE 3: A next-generation heavy-ion experiment at the LHC", `arXiv:2211.02491 [physics.ins-det]`.